iScience, Volume *24*

Supplemental information

Hydra vulgaris shows stable responses to thermal stimulation despite large changes in the number of neurons

Constantine N. Tzouanas, Soonyoung Kim, Krishna N. Badhiwala, Benjamin W. Avants, and Jacob T. Robinson

Supplemental Data

Fig. S1. **Temperature profile and calcium trace of three representative *Hydra* stimulated at 30ºC, related to Fig. 3 and "Transparent Methods: Analysis of neural activity in the peduncle of *Hydra*"**

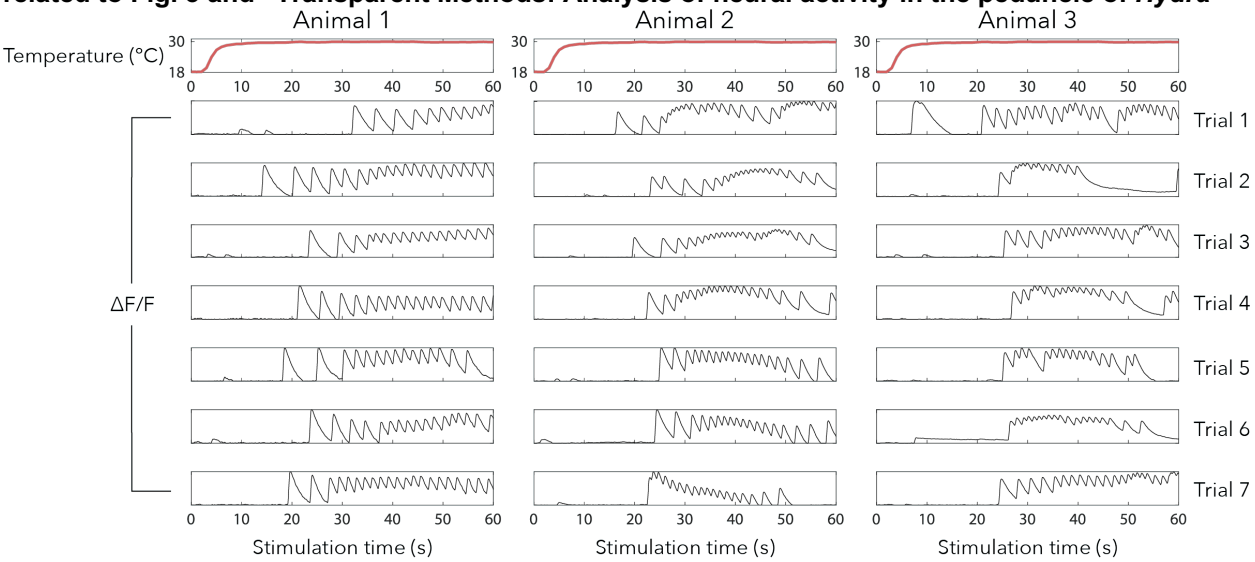

The temperature of the device plateaus approximately 5 seconds after the start of the temperature change, and the median time to the start of a contraction burst is 24 seconds after the start of the temperature change.

Fig. S2. **Day-to-day variation in intra-animal neural activity, related to Fig. 3**

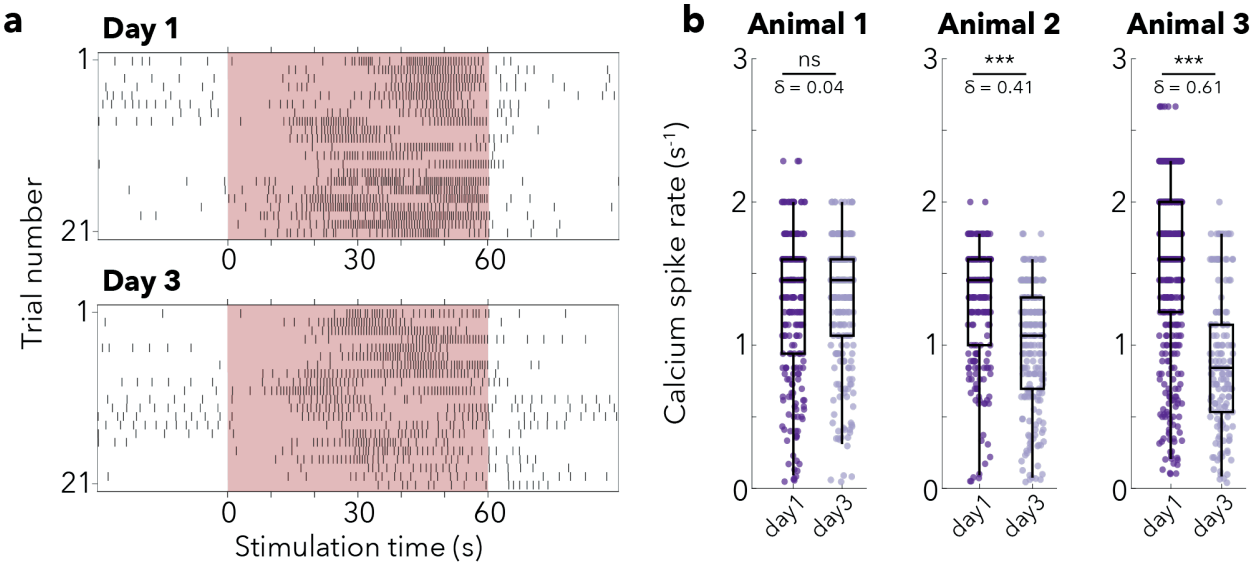

a Raster plot of *Hydra* stimulated at 36ºC on Day 1 and Day 3 (t = 48 hours after the previous stimulation on Day 1). **b** Calcium spike rate comparison between Day 1 and Day 3 for individual animals (Mann-Whitney U test, ns = not significant, *** p<0.0001, δ = Effect size using Cliff's delta). Box-and-whisker plots indicate Q1, median, and Q3; whisker lengths indicate the 2nd and 98th percentiles.

Fig. S3. **Differences in neuron counts due to *Hydra*'s natural size variations, related to Fig. 4**

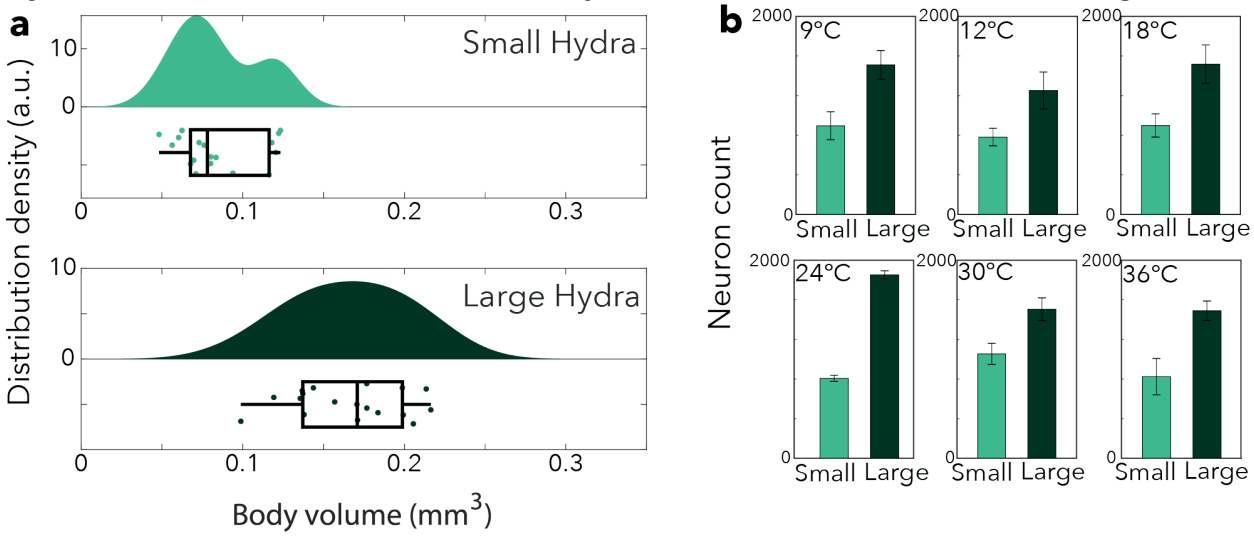

a Size distribution of small and large *Hydra*. Box-and-whisker plots indicate Q1, median, and Q3; whisker lengths indicate whisker lengths indicate the 2nd and 98th percentiles. **b** Comparison of neuron count between small and large *Hydra* groups at each stimulation temperature. (N=3 per size at each temperature). Data represented as mean +/- standard error of the mean.

Fig. S4. **Bootstrapping analysis on spike rates of whole and bisected Hydra, related to Fig. 5**

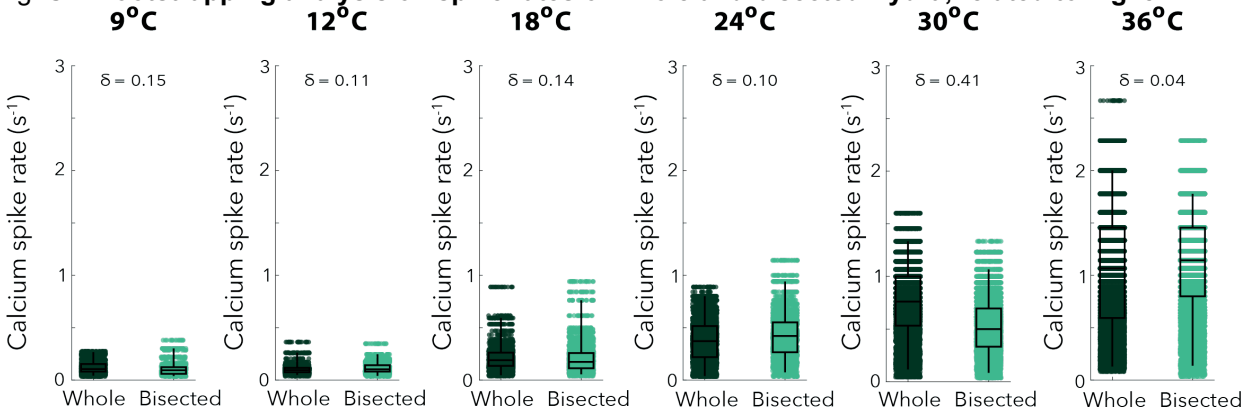

Comparison of bootstrapped calcium spike rates of whole and bisected *Hydra*. Box-and-whisker plots indicate Q1, median, and Q3; whisker lengths indicate whisker lengths indicate the 2nd and 98th percentiles.

Transparent Methods

Microfluidic device fabrication:

All microfluidic devices were fabricated using polydimethylsiloxane (PDMS) (Sylgard 184). The thermal stimulation chip is a two-layer device: bottom stimulus flow channels and a top *Hydra* immobilization chamber, separated by a glass coverslip. By separating *Hydra* from fluid flow, the animal can be rapidly heated/cooled (by flowing water at controlled temperatures through the bottom stimulus flow channels) without undesired mechanical stimulation from high flow rates (avoided due to the glass coverslip separation). To construct the double layer chip, we first fabricated the top immobilization layer by molding PDMS from a master mold adapted from a 2 mm diameter x 100 µm tall chemical perfusion chip (designed as previously described) (Badhiwala *et al.*, 2018). Briefly, a circular observation chamber designed specifically for *Hydra* was patterned using soft lithography on a silicon substrate, and a ~5mm thick layer of PDMS was molded from this master mold. After punching holes for the inlet and outlet ports with a 1.5mm diameter biopsy punch, the immobilization layer was O_2 plasma bonded to a 12mm diameter glass coverslip.

This top immobilization chip was then placed with a glass coverslip side facing down directly on the center of the master mold for the flow layer. Uncured PDMS was poured into the flow layer mold surrounding the immobilization chamber, taking care not to clog the ports in the immobilization layer. The master mold for the flow layer (adapted from Duret et al (Duret *et al.*, 2019)) was 3D-printed with 1mm tall channels (Form 2, Flexible Resin, Formlabs). After curing the PDMS for the bottom flow layer (thereby embedding the immobilization chamber), holes were punched for inlet/outlet access for the flow layer. Finally, this double layer microfluidic chip was O_2 plasma bonded to a 500 µm fused silica wafer (University Wafer).

After unloading *Hydra* from the device at the end of a trial (see "Loading and unloading *Hydra*"), both layers of the microfluidic device were rinsed with *Hydra* media (media adapted from the laboratory of Robert Steele), sonicated in *Hydra* media for at least 10 minutes, and soaked at room temperature in *Hydra* media. Such cleaning allowed for devices to be reused across multiple days of trials.

Hydra strains and maintenance:

All trials were conducted on transgenic lines with neuronal expression of GCaMP6s, developed with embryo microinjections by Christophe Dupre in the laboratory of Dr. Rafael Yuste. *Hydra* were cultured using the protocol adapted from the laboratory of Robert Steele (UC Irvine). *Hydra* were raised at either 18ºC or 25ºC in incubators, both with 12:12 hours of light:dark cycle. Animals were fed freshly hatched *Artemia* nauplii (Brine Shrimp Direct) three times a week and cleaned after approximately 4 hours with fresh *Hydra* media. All animals used in trials were starved for a day prior to thermal stimulation experiments and were not re-used.

Loading and unloading *Hydra*:

Hydra were loaded into the inlet port of *Hydra* enclosure using a 10 mL syringe with attached tygon tubing. *Hydra* were then pulled a couple of centimeters into the tygon tubing before the tubing was inserted into the inlet port of the microfluidic device. By applying gentle pressure and gently pulsing on the plunger of the syringe, *Hydra* could be successfully loaded into the immobilization chamber without damage from mechanical shear. After the experiments, *Hydra* were removed from the device by applying pressure on the plunger of a tygon tubing-attached syringe and flushing the organism out the outlet port.

Thermal stimulation assay

After loading *Hydra*, two programmable syringe pumps (New Era NE-500) controlled by an Arduino Mega ADK were used to drive the flow of deionized water at a rate of 6 mL/min through two inlet ports of the thermal stimulation device. The third inlet port was connected to an additional syringe (useful for removing air bubbles when initially filling the bottom stimulus flow channels prior to the start of a trial), and the device outlet port was connected to a water collection container. Fluid flow from the two pumps was heated/cooled using two in-line heaters (SC-20, Warner Instruments) regulated by a Dual Channel Bipolar Temperature Controller (CL-200A, Warner Instruments). One in-line heater supplied *Hydra*'s culture temperature during control periods (i.e. 18°C or 25°C), while the other heater supplied the desired stimulus temperature of a given trial (i.e. 9°C, 12°C, 18°C, 24°C, 25°C, 30°C, or 36°C). To compensate for heat exchange between water flowing through inlet tubing and the environment, a FLIR ONE thermal camera

was used to calibrate the relationship between in-line heater temperature settings and actual temperatures of the thermal stimulation device.

Each thermal stimulation trial began with two minutes at *Hydra*'s culture temperature. Subsequently, the trial alternated between stimulus periods (single temperature for a given trial; 9°C, 12°C, 18°C, 24°C, 25°C, 30°C, or 36°C) and control periods (based on *Hydra*'s culture temperature; 18°C or 25°C). Stimulus periods always lasted for 60 seconds, while control periods varied in length between 30 and 90 seconds in 15 second increments, to help distinguish between stimulus-evoked responses and spontaneous activity. The lengths of control periods were randomly ordered and averaged to 60 seconds over the course of a trial. For a visual representation of thermal stimulation protocols, see Fig. 3a. The timing of transitions between stimulus and control periods were recorded through the Arduino's Serial Monitor (57600 baud rate) and used to determine portions of recordings corresponding to stimulus and control periods. For experiments on size comparison of *Hydra* cultured at 18°C, 3 large and 3 small animals for each temperature (9°C, 12°C, 18°C, 24°C, 30°C, and 36°C), 36 animals in total were used. For *Hydra* cultured at 25°C, 3 animals were used at 18°C, and 4 animals at 25°C, 30°C, and 36°C over the course of 7 days.

Fluorescence imaging for GCaMP6s was conducted on a Nikon SMZ18 stereomicroscope with a SHR Plan Apo 2x objective (0.3 NA) and Andor Zyla 4.2 (16 fps, 3x3 image binning). Excitation was provided by a X-Cite Xylis XT720L at 50% intensity through a Chroma EGFP filter cube (catalog no. 49002). The start of fluid flow using Arduino and the start of recording using Andor Solis were manually synced with a maximum delay less than 0.5 seconds.

Measuring Day-to-Day Variability in Calcium Spike Rate

To better understand the source of variability in our data we asked how much of the difference in calcium spike rates could be explained by day-to-day variability in the same animal. To answer this question, we stimulated the same whole *Hydra* twice at 36ºC over a 48 hours interval (N=3 organisms) - the same time interval between the whole and partial *Hydra* experiments. We found that while one animal maintained its spike rate with no statistically significant difference, two animals had a statistically significant decrease in spike rate, even when stimulated at the same temperature before and after the 48-hour difference (Fig. S2b). Accompanying effect sizes measured using Cliff's delta (δ) ranged from 0.04 for first animal to 0.41 and 0.61 for the latter two (overall pooled effect size of 0.35), contextualizing the relative magnitudes of observed experimental effects against typical day-to-day variability in *Hydra*.

Longitudinal imaging of the entire nervous system

Transgenic *Hydra vulgaris* AEP expressing GFP (green fluorescent protein) in their interstitial cell lineage were used to investigate how the number of neurons varies with animal size and nutrient availability. Animals with large body size (>2 mm long) at the beginning of the study were starved for the duration of the experiment. A control group of animals with small body size (< 1mm) at the beginning of the study were fed with an excess of freshly hatched *Artemia nauplii* three times a week. Size of the animal was defined as the length of the animal in a relaxed state (between fully contracted and fully elongated). *Hydra* media was replaced daily for all animals.

Volumetric imaging was performed using a confocal microscope (Nikon TI Eclipse) with animals immobilized in chemical perfusion microfluidic chips (see Badhiwala et al. (Badhiwala *et al.*, 2018)) and chemically paralyzed with 1:5000 linalool. Animals were imaged three times a week (one day after the control animals were fed) over two weeks. All images were acquired with a 10x DIC objective. The majority of the images were acquired with 1024 x 1024 pixels (x, y) resolution and 5 mm z-resolution. A lower resolution of 512 x 512 pixels and 10 mm z-resolution were used in a few cases to speed up volumetric imaging where micromotions of the animals could not be completely eliminated with chemical anesthetic (becoming increasingly important with animals starved for extended periods of time).

To quantify the total number of neurons, a maximum intensity projection image was generated from the z-stacks. After binarizing the resulting image with a user-defined threshold, individual regions (or neurons) were summed to determine the total number of neurons. However, due to anatomical overlap of multiple neurons in high-density regions such as the peduncle, future work will focus on developing transgenic animals that express fluorescent reporters in the nuclei of specific neural cell types, rather than in the cytosol of interstitial cell derived lineages (as in the animals used here).

To quantify the body size during an experiment, we binarized the maximum intensity projection image with a lower threshold than above. Filling holes in the binarized image produced the binary mask for

the whole animal. Body size was calculated as the area of this binary region, and body volume was body size times the thickness of the immobilization chamber (160 μm).

The duration of the experiment was kept under two weeks, as well-fed animals can reproduce asexually by budding every 3-4 days. In fact, one of the animals in the well-fed group began forming a bud on day 10 of the experiment. Additionally, as animals are starved, they become smaller and more transparent, making them difficult to handle. In our starved group, we 'lost' one of the animals on day 15 as it was either too transparent or had shrunk considerably to not be discerned from the plate.

Creating bisected *Hydra*

For the purpose of investigating whether the number of neurons affect the neural response to thermal stimulation in *Hydra*, the animals were cut along the oral - aboral axis in order to ensure we have a significantly different distribution of body size while retaining tentacles, the hypostome, body column, and peduncle. Whole, uncut *Hydra* were imaged on day 1 as the same protocol described above. Then each *Hydra* was cut along the oral-aboral axis under a dissection microscope using an X-acto knife (#2 knife with #22 blade). The cut animals were incubated in separate 24-well compartments and were fed the day after being cut (day 2) to keep the feeding schedule consistent. After letting them recover for 48 to 50 hours, they were thermally stimulated again under the same condition they were exposed to before being cut. Five animals were used for each stimulation temperature. For the comparison of neural response between whole and bisected *Hydra*, only one of the two bisected *Hydra* was used.

Behavioral analysis

DeepLabCut (Nath *et al.*, 2019) along with custom MATLAB code was used to quantify *Hydra*'s behavioral responses to thermal stimuli. 20 frames per video were extracted for manual tracking according to k-means clustering on DeepLabCut. *Hydra* in each frame was then manually annotated with the locations of the basal disc (aboral end), left side, center, and right side of the body, and hypostome (oral end). Two corners of the immobilization chamber were additionally annotated, providing a known distance (2 mm) to convert pixel measurements to micrometer measurements. The annotated dataset was used as training data for DeepLabCut. After evaluating the model, the videos were analyzed using the trained model which yielded the coordinates of the seven points listed above for every frame (total of 14,600 frames) for every video, along with annotated videos. With the coordinates obtained from DeepLabCut annotations, body width was calculated as the sum of the distance from the left side to the middle of the body and the distance from the middle to the right side of the body, and body length was calculated as the sum of the distance from the hypostome to the middle of the body and the distance from the middle of the body to the basal disc (Fig. 2b, bottom panel) with a custom MATLAB code.

Analysis of neural activity in the peduncle of *Hydra*

To determine the timing and frequency of calcium spikes in *Hydra*'s peduncle oscillator, fluorescence microscopy recordings from thermal stimulation trials of neuronal GCaMP6s *Hydra* (see "Thermal Stimulation Assay") were processed in Fiji (ImageJ) (Schindelin *et al.*, 2012) and in MATLAB. For each frame of the recording, Fiji was used to calculate the average intensity of a ROI encompassing *Hydra*'s peduncle and aboral regions (same ROI for the entire recording). In MATLAB, this intensity trace was smoothed (5 data point span), and the built-in findpeaks function was used to determine calcium spike locations based on their prominence in the intensity traces (see Movie S1, Movie S2, and Fig. S1 for representative calcium traces). Spurious spikes (e.g. from measurement noise) were eliminated by additionally testing that each identified calcium peak was the only local maximum exceeding a threshold prominence value within a narrow window of the peak.

Raster plots were then directly produced from the times of peduncle oscillator spikes during each stimulus period and the surrounding 30 seconds at culture temperature. Peristimulus time histograms (defined as calcium firing rate) were calculated by counting the number of spikes across all stimulus periods at a given stimulation temperature in a 10-second sliding window, then normalizing by the number of stimulus periods and the length of the window. Instantaneous calcium spike rates for a given thermal stimulus temperature were defined as the inverse of the amount of time elapsed between two successive calcium spikes during stimulus periods. We highlight that apparent discretization of instantaneous calcium spikes at high rates stems from discrete sampling intervals (i.e., frames in a microscopy video) to measure a continuous underlying process (i.e., calcium dynamics in a GCaMP6s-expressing neuron). At these relatively high firing rates, a small integer number of frames elapsed between peaks would cause apparent

discretization of a continuous process. For instance, 8 frames elapsed between spikes in a 16 fps recording would correspond to a calcium spike rate of 2/sec. The next slowest measurable increment 16 fps would be a calcium spike rate of 1.78/sec, arising from 9 frames elapsed between spikes, and so on for other integer counts of elapsed frames.

Estimating the value of Q_{10} of tCB neurons

The thermal coefficient, Q_{10}, was calculated to elucidate one possible biophysical mechanism behind the temperature dependent calcium spike rates using Eq. 1 (see Evaluation of mechanisms of the temperature-dependent calcium spike rate in Results). T_1 is 18ºC, and R_1 is the median calcium spike rate at T_1. T_2 ranges from 18ºC to 36ºC, and R_2 is the corresponding median calcium spike rate at T_2. As the nature of Eq. 1 is in the form of an exponential, we took log in the y axis, plotting a log-linear plot of $\log(R_2/R_1)$ vs. (T_2-T_1). Using the polyfit function in MATLAB, we fitted the data points to a linear equation to determine the slope. The value of Q_{10} was then calculated using the obtained slope.

Statistical analysis

To determine statistical significance between the calcium spike rates across temperatures, two-sided Wilcoxon rank sum test (equivalent to Mann-Whitney U-test) was implemented using the ranksum function in MATLAB. The test returns the p-value with the null hypothesis that the data points in the two datasets to be samples from distributions (whether continuous samples, or discrete and ordinal samples) with equal medians (Lehmann, 1951; Fay and Proschan, 2010). This test also allows the two data sets to have different lengths. This particular test was chosen because of the nature of length-variant distribution of calcium spike rates, of which we consider the median, not the mean, for comparison.

We also used Cliff's delta (Cliff, 1993), which represents the effect size that gives a quantitative measurement of the difference between two groups of data. We chose to use Cliff's delta because of its neutrality to mean values, as it takes the entire distribution into account. Let $X = \{x_1, \ldots, x_m\}$ and $Y = \{y_1, \ldots, y_n\}$ be the two samples of interest. Defining d as follows,

$$d(i,j) = \begin{cases} +1, & x_i > y_j \\ -1, & x_i < y_j \\ 0, & x_i = y_j \end{cases}$$

Cliff's delta (δ) can be calculated as

$$\delta = \frac{1}{mn} \sum_{i=1}^{m} \sum_{j=1}^{n} d(i,j)$$

where $-1 \leq \delta \leq +1$. The absolute δ values that are closer to 1 indicate larger differences between the samples, while the values closer to 0 indicate small differences between the samples.

We also performed statistical bootstrapping to randomly pool distributions of calcium spike rates from whole and bisected Hydra (N=5) in order to quantify statistical difference between the two groups. As per protocol (see "Thermal stimulation assay" in Transparent Methods), each animal was stimulated 7 times at a given temperature. We pooled calcium spike rates from 7 stimulation periods across the aforementioned 5 animals to create one artificial animal so that at least one stimulation period from each of the animals would be included. This process was done 100 times to create the calcium spike rates shown in the Fig. S3.

Supplemental References

Badhiwala, K. N. et al. (2018) ‘Microfluidics for electrophysiology, imaging, and behavioral analysis of: Hydra’, *Lab on a Chip*. Royal Society of Chemistry, 18(17), pp. 2523–2539. doi: 10.1039/c8lc00475g.
Cliff, N. (1993) ‘Dominance statistics: Ordinal analyses to answer ordinal questions.’, *Psychological Bulletin*, 114, pp. 494–509.
Duret, G. et al. (2019) ‘Magnetic Entropy as a Proposed Gating Mechanism for Magnetogenetic Ion Channels’, *Biophysical Journal*. Cell Press, 116(3), pp. 454–468. doi: 10.1016/J.BPJ.2019.01.003.
Fay, M. P. and Proschan, M. A. (2010) ‘Wilcoxon-Mann-Whitney or t-test? On assumptions for hypothesis tests and multiple interpretations of decision rules’, *Statistics surveys*, 4, pp. 1–39. doi: 10.1214/09-SS051.
Lehmann, E. L. (1951) ‘Consistency and Unbiasedness of Certain Nonparametric Tests’, *The Annals of Mathematical Statistics*. Institute of Mathematical Statistics, 22(2), pp. 165–179. Available at: http://www.jstor.org/stable/2236420.
Nath, T. et al. (2019) ‘Using DeepLabCut for 3D markerless pose estimation across species and behaviors’, *Nature Protocols*, 14(7), pp. 2152–2176. doi: 10.1038/s41596-019-0176-0.
Schindelin, J. et al. (2012) ‘Fiji: an open-source platform for biological-image analysis’, *Nature Methods*, 9(7), pp. 676–682. doi: 10.1038/nmeth.2019.